24th COBEM - 2017

24th ABCM International Congress of Mechanical Engineering
December 3-8, 2017, Curitiba, PR, Brazil

COBEM-2017-0566
CFD MODELLING OF DELFT III FLAME UNDER ACOUSTIC FORCING

Rígel F. do C.
Alex Álisson B. S.
SENAI CIMATEC – Integrated Campus of Manufacture and Technologies | Salvador, Brazil
rigel.fc@outlook.com, alex.santos@fieb.org.br

Abstract: *This article will attempt to investigate acoustic forcing in 'Delft Flame III' – a turbulent, pilot-stabilized, diffusive, non-luminous, natural gas flame – using Ansys Fluent. Geometry is modelled as a two-dimensional, axisymmetric, structured Cartesian mesh; pilot holes' influence is neglected. Reynolds Stress is used as turbulence model, Discrete Ordinates as radiation model and Weighted Sum of Grey Gases for the absorption coefficient calculation. Inlet fuel is simplified as comprised solely of methane and molecular nitrogen, whose compositions are adjusted as to preserve the original calorific value of the Dutch natural gas; far field is modelled as symmetry and outlet as zero-gauge pressure (with standard air at ambient conditions set as backflow configuration). Three chemical mechanisms are used and compared: GRI 3.0, UCSD 2016-12-14 and Narayanaswamy et. al. 2014.; results obtained were equivalent, except for NO mass fraction and for the soot volume fraction. Similarly, two combustion models were tested: Steady and Unsteady Laminar Flamelet; the former was sufficient to reach converged results for all variables involved (apart from H_2 and CO mass fractions), however the latter decreased the accuracy of NO and soot results. Finally, the software revealed to be uncappable of running a transient analysis from the steady-state, converged solution.*

Keywords: *Delft Flame III, combustion, Computational Fluid Dynamics (CFD), acoustic forcing*

1. INTRODUCTION

"Delft III" is the designation assigned to a turbulent, pilot-stabilized, diffusive, nonluminous, natural gas flame of high interest worldwide, such that it has been under academic investigations roughly for the past 20 years and is a target case in the series 'International Workshop on Measurements and Computations of Turbulent Non-Premixed Flames (TNF)' (SNL, 2003). In parallel to that, it has already been stablished at literature that submitting combustion flames to acoustic excitation brings many benefits, e.g. smaller pollutant emissions and fuel consumption (Rocha, 2007; Santos, *et al.*, 2011). Under these circumstances, the aim of this paper is to numerically investigate how Delft III burner would perform under such excitations – what, to the best of the authors' knowledge, is novel.

One of the benefits of choosing such flame is the experimental data available – for the computational model validation purposes (SNL, 2003; except for soot, measured by Qamar, *et al.*, 2009) – and the vast numerical investigations conducted on it so far by the literature; all of them, however, for a "regular" – non-acoustically excited – operation of the flame. And given this work will be about predicting the acoustically forced results, for which no experimental data is available yet, it was decided to work with models' (vg. turbulence) standard coefficients and not to modify the geometry or boundary conditions (as done by Naud, *et al.*, 2007).

Nomenclature

CFD	Computational Fluid Dynamics	DOM	Discrete Ordinates Model
k	turbulence intensity	LDA	Laser Doppler Anemometry
LII	Laser-Induced Incandescence	MOM	Method of Moments
P1	spherical harmonics' simplest model	PDF	Probability Density Function
RRLIF	Raman Rayleigh Laser-Induced Fluorescence	RSM	Reynolds Stress Model
SIMPLE	Semi-Implicit Method for Pressure-Linked Equations	SLFM	Steady Laminar Flamelet Model
SRI	Soot Radiation Interaction	SST	Shear Stress Transport
TCI	Turbulence Chemistry Interaction	TRI	Turbulence Radiation Interaction
uSLFM	Unsteady Laminar Flamelet Model	WSGGM	Weighted Sum of Grey Gases Method
ω	turbulence's specific dissipation rate		

2. COMPUTATIONAL PROCEDURE

The burner features a well-known geometry and operating conditions (Peeters, *et al.*, 1994):

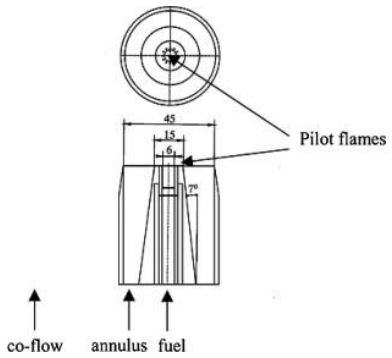

Figure 1: Burner's top and cross views.

Table 1 – Burner's operating conditions.

inlet jet	property	value	unit
fuel	U	21,9	m/s
	T	295	K
	Re	9700	
annulus	U	4,4	m/s
	T	295	K
	Re	8800	
coflow	U	0,4	m/s
	T	295	K

A comprehensive explanation of the burner's idiosyncrasies can be found at Naud, *et al.* (2007). To ensure an efficient computational usage, a two-dimensional, axisymmetric, structured Cartesian mesh was generated (Merci, *et al.*, 2005; Roekaerts, *et al.*, 2006), by means of the open-source software Gmsh 2.16.0 (Geuzaine and Remacle, 2009):

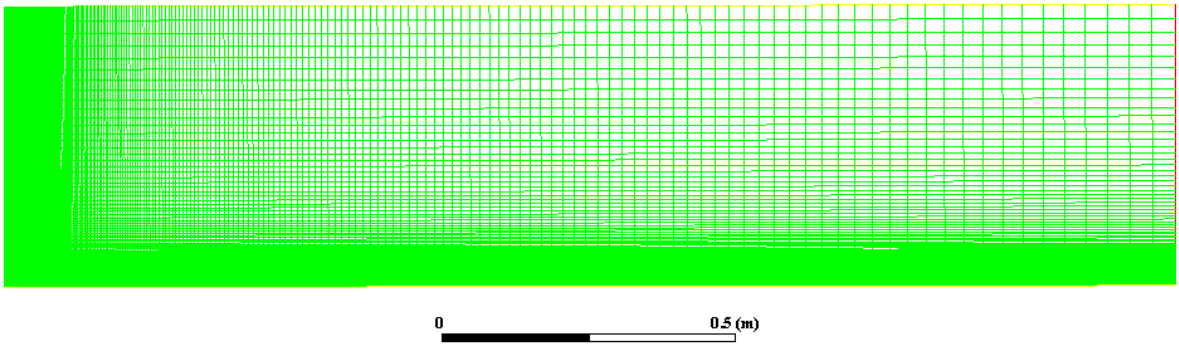

Figure 2: Simulation's mesh.

Although the burner's geometry is not exactly axisymmetric, the flow becomes axisymmetric few millimeters above the rim, such that experimental measurements were collected – and the literature's numerical results presented – for the axial and radial directions only. At the present work's computational domain, such directions are respectively fixed as (*D* being the fuel inlet's diameter) 1.5 m (or 250D, as in Reddy, *et al.*, 2015) and 36 cm (or 60D, as in Naud, *et al.*, 2007) – the combination of the biggest values used for each of them at the consulted references. Mesh details are:

Table 2 – Mesh specifications.

direction		# cells	average mm / cell	% increase towards far-field
axial		250	6,000	2,0
radial	fuel	15	0,200	
	wall	2	0,223	
	pilot ring	1	0,107	
	wall	15	0,263	
	annulus	50	0,300	0,5
	coflow	75	4,500	5,5
	TOTAL	*158*	*2,278*	-

From this point onwards, activities were done in proprietary software Ansys Fluent 17.1.

The fuel, annulus and coflow inlet streams' boundary conditions are the velocity profiles specified at SNL, 2003. Given this flame has been studied in different places worldwide, literature has stablished a simplified, "standard" fuel composition which allows for an accurate comparison of results, while maintaining the original calorific value:

Table 3 – Experimental and numerical fuel volumetric compositions.

Species		**Volumetric Composition**	
formula	**Name**	**experimental**	**numerical**
CH_4	methane	0,8129	0,853
C_2H_6	ethane	0,0287	
C_3H_8	propane	0,0038	
C_4H_{10}	butane	0,0015	
C_5H_{12}	pentane	0,0004	
C_6H_{14}	hexane	0,0005	
N_2	nitrogen gas	0,1432	0,147
O_2	oxygen gas	0,0001	
CO_2	carbon dioxide	0,0089	

Under these circumstances, the numerical fuel's stoichiometric mixture fraction is 0,07, the same as the experimental one (Kim, 2004). The pilot flames, on their turn, are neglected in the calculations (Habibi, *et al.*, 2007).

The domain's outlet is set as zero-gauge pressure; inlet streams do not feature pressure differences from atmospheric conditions either (Habibi, *et al.*, 2007). Finally, the lateral border is modelled as symmetry (as in Reddy, *et al.*, 2015).

Turbulence

The simulation started with the *Shear Stress Transport* (SST) k-ω model for turbulence, and then switched to *Reynolds Stress* (also referred to as *Second Order* or even *Second Moment Closure*) *Model* (RSM) (Reddy, *et al.*, 2015) – *Baseline* (BSL) submodel – once an initial, converged solution was obtained.

Radiation

As in the previous topic, the simulation started with P1 model (Yadav, *et al.*, 2013), and then switched to *Discrete Ordinates Model* (DOM) (Habibi, *et al.*, 2007). The solid angle's discretization inputs are summarized in the table below:

Table 4 – Solid angle's specifications.

parameter	**direction**	
	θ	**φ**
angles	2	2
pixels	1	1

Increasing the above numbers was observed not to interfere with the results. Finally, the mixture's absorption coefficient is calculated by the *Weighted Sum of Grey Gases Method* (WSGGM) (Reddy, *et al.*, 2015), the scattering coefficient is kept as zero (as scattering can be neglected) and the refractive index is set to unity (Habibi, *et al.*, 2007).

Chemistry

As per Reddy, *et al.* (2015) and Habibi, *et al.* (2007), mapping scalars – most notably, the mixture fraction – are used to indirectly model the diffusion and reaction of species across the domain. Turbulence-chemistry interactions (TCI) are accounted for by means of a presumed β-*Probability Density Function* (PDF). The instantaneous flame structure is computed by the *Steady Laminar Flamelet Model* (SLFM); once the simulation has converged, a parallel run of the Unsteady Laminar Flamelet Model (uSLFM) shall be executed.

Reaction Mechanism

Three chemical kinetics (*chemkin*) mechanisms were analyzed:

Table 5 – Chemical mechanisms used in the present work.

name	**version**	**number of**	
		species	**reactions**
GRI-Mech (Smith, *et al.*)	3.0	53	325
University of California at San Diego (UCSD, 2016)	2016-12-14	57	268
Narayanaswamy, *et al.*, 2014	2014	255	1509

Results presented will, in case of disparities, specify from which model they were obtained. Albeit being old, GRI has been included because it is still the base for Fluent's built-in methane-air mechanism. The authors also tried to use Polytechnic University of Milan's (Ranzi, *et al.*, 2014) and Narayanaswamy, *et al.*, 2015's complete mechanisms, but they failed to compile at Fluent.

Pressure-Velocity Coupling

Is implemented by the *Semi-Implicit Method for Pressure-Linked Equations* (SIMPLE) algorithm (Merci, *et al.*, 2006).

Spatial Discretization

The simulation started with a first-order upwind scheme for turbulence and radiation related parameters, and then improved afterwards, so that all variables are calculated by a second-order scheme at the final solution (Reddy, *et al.*, 2015).

NOx

Thermal, prompt and intermediate (N_2O) formation mechanisms are considered, as well as NOx reduction due to reburning. Both O and OH contributions are calculated by the instantaneous approach; N_2O is modelled by the transported-simple way, such that its individual mass fraction results are visible. As in Habibi, *et al.* (2007), reduction is accounted for via the partial-equilibrium approach – with methane as reburning fuel, of unity equivalence ratio – and NOx-turbulence interaction via the PDF mixture fraction.

However, as diagnosed by Habibi, *et al.* (2007), accurate NO predictions can only be obtained from full *Turbulence Radiation Interaction* (TRI), what is presently unavailable in Fluent. Hence results obtained are expected to show strong deviations from measurements.

Soot

The *Method of Moments* (MOM) is supposed to be the preferred option for soot calculations in flames, but its implementation in Fluent still misses features already used by literature (see e.g. Mueller and Pitsch, 2012) and was observed to return poor results in the present work (even after increasing the number of moments being solved for). In this case, the Moss-Brokes Model is used instead (as in Reddy, *et al.*, 2015).

Acetylene and ethylene are included as precursors and surface growth species. As in the NOx configuration, turbulence interaction is accounted for via the PDF mixture fraction and species are calculated by the instantaneous approach. Finally, soot oxidation is computed by Lee model and *Soot Radiation Interaction* (SRI) is accounted for.

Simulation Workflow

The simulation's final configuration was reached through the following path:

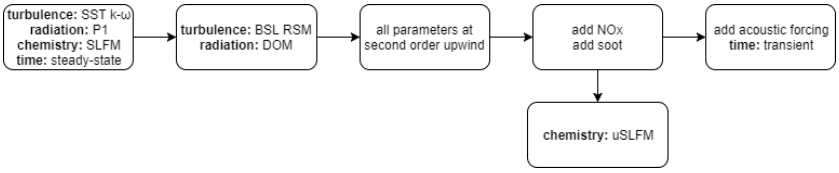

Figure 3. Simulation's flowchart.

Lastly, all configuration details not expressly mentioned above are the software's standard ones.

3. RESULTS AND DISCUSSION

Fluent's *Theory Guide* – topic 4.1.1 (namely *Turbulence* > *Underlying Principles of Turbulence Modeling* > *Reynolds (Ensemble) Averaging*) – is unclear as whether the software automatically switches from *Reynolds* (or *Time* or even *Ensemble*) averaged to *Favre* (or *Mass*) averaged Navier-Stokes equations when the flow density is observed to change, hence which "version" of the results the user is getting. This has implications towards the validation of the simulation, since part of Delft III's experimental data (SNL, 2003) is provided in both formats and numbers can differ considerably between them. Based on literature and on other topics of that same Guide, it will be assumed that the code does switch automatically, thus numerical results will – when that is the case – be compared against the Favre-averaged experimental data.

At the below figures, lines are numerical results and symbols are experimental measurements. Heights above the burner rim are distinguished by colors: blue for 5 cm, green for 10, red for 15, purple for 20 and orange for 25 cm.

Static Flame Operation

The following initial set of variables are the ones whose experimental measurements were done via *Laser Doppler Anemometry* (LDA):

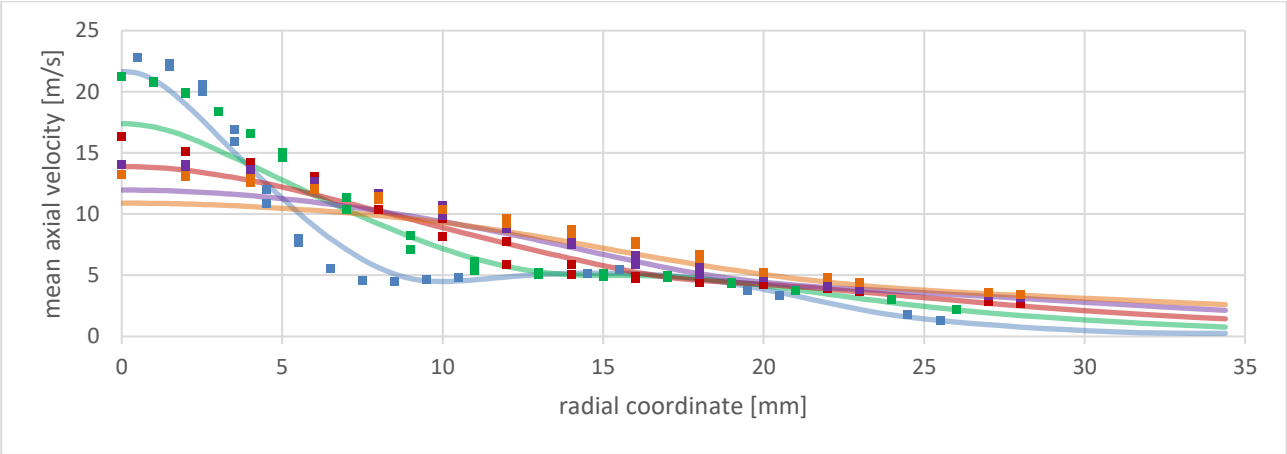

Figure 4. Mean axial velocity profiles at different heights above the burner.

The solver underpredicts the mean axial velocity close to the burner's axis, mostly near its surface (where TCI is stronger). References like Reddy, *et al.* (2015) found more accurate values, but they have implemented the setup modifications it was decided above (see 1. **INTRODUCTION**) not to go with.

For the mean radial velocity, on its turn, it is necessary to plot their absolute value, as experimental measurements collected either positive or negative results (depending upon the side of the flame where the instrument was positioned at the time):

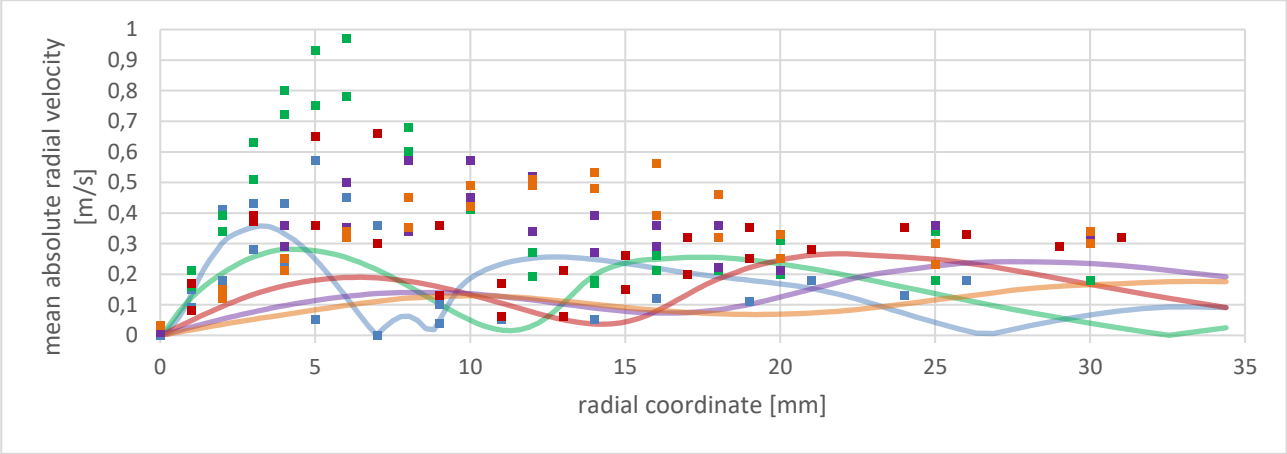

Figure 5. Mean absolute radial velocity profiles at different heights above the burner.

And those highly oscillating measurements reveal how difficult it is to analyze the radial velocity in this flame. In general, the solver succeeded in capturing overall trends, but underpredicted peak values.

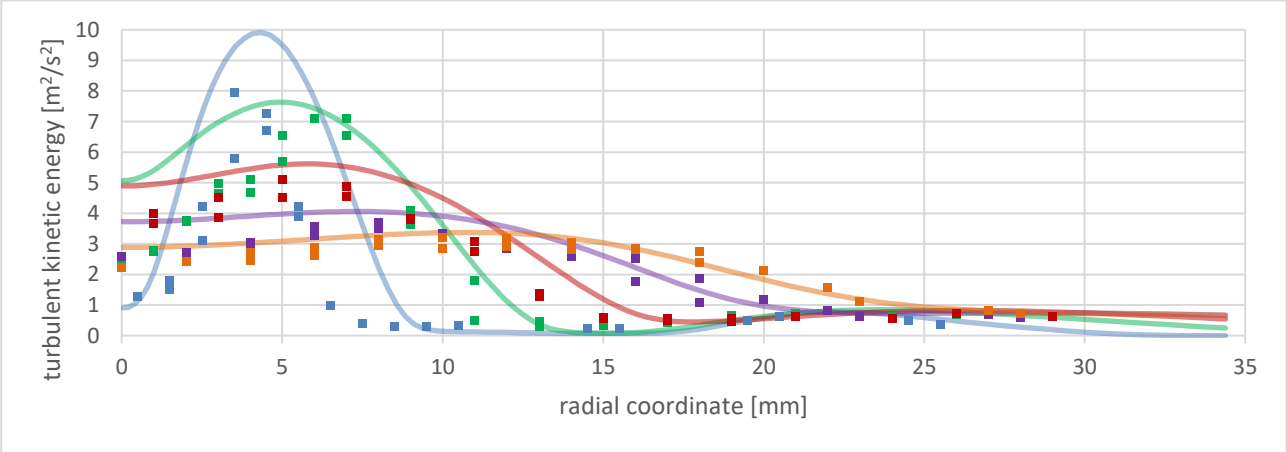

Figure 6. Turbulent kinetic energy profiles at different heights above the burner.

Again, here discrepancies from experimental measurements are stronger closer to the burner's axis and surface. The solver overpredicts turbulence, both in peak values and in decay intensity; what is, however, expected from – and related to – the underpredicted velocities in the same region: a slower local flow gives rise to stronger recirculations.

The variables from this point onwards are the ones whose experimental measurements were done via Favre-averaged *Raman Rayleigh Laser-Induced Fluorescence* (RRLIF):

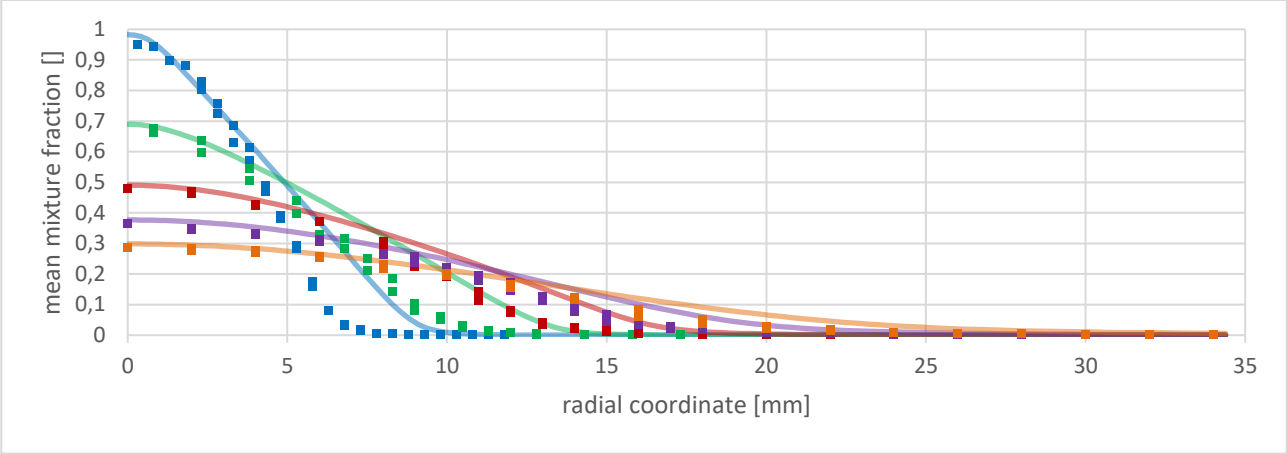

Figure 7. Mean mixture fraction profiles at different heights above the burner.

The solver underpredicts the intensity with which the mean mixture fraction decays as you depart from the burner's axis, but peak values are in good agreement with the experiments. Results shown up to this point suggest that the numerical solution predicts a thicker, slower flame than the real one.

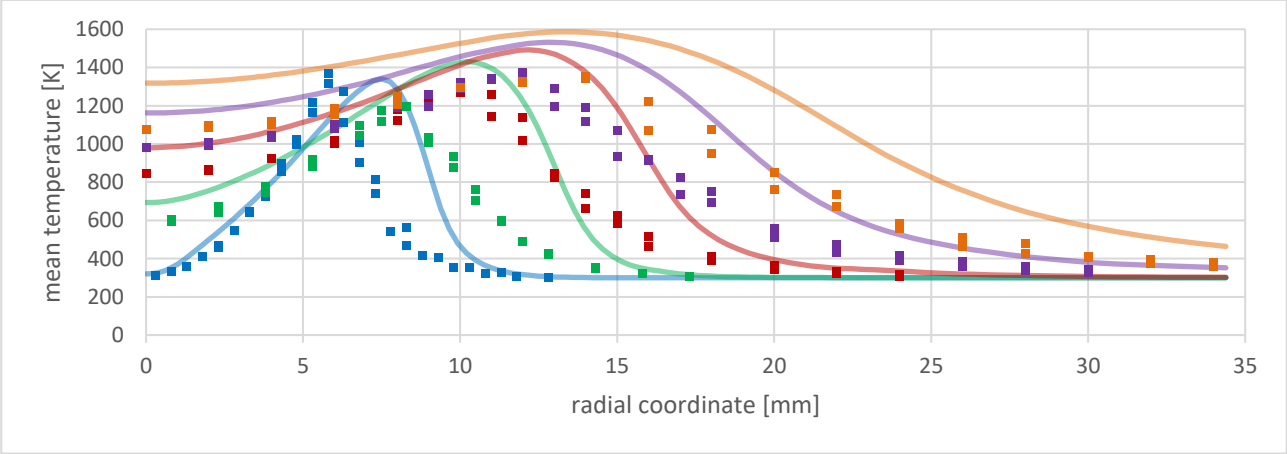

Figure 8. Mean temperature profiles at different heights above the burner.

The thicker flame hypothesis becomes stronger when results for mean temperature are analyzed: the solver indeed overpredicts peak values, while underpredicts their decay rates; i.e. a thicker and longer flame.

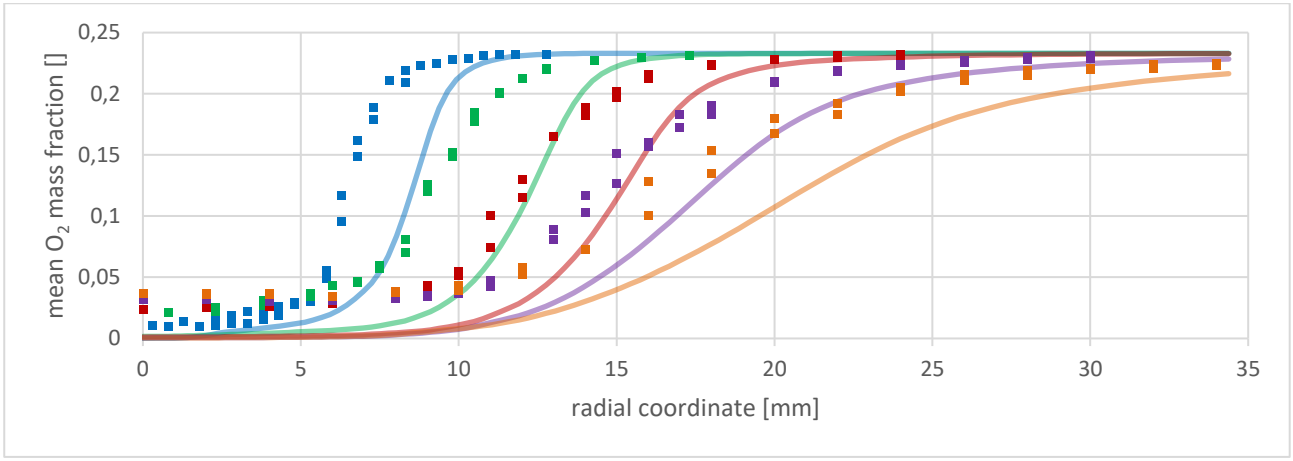

Figure 9. Mean O_2 mass fraction profiles at different heights above the burner.

Despite experimental O_2 mass fraction results should not be used for comparison against numerical data (SNL, 2003), they have been included here for the sake of completion. And they seem to corroborate the thicker & longer flame hypothesis: the computational flame takes longer – on both axial and radial directions – to extinguish.

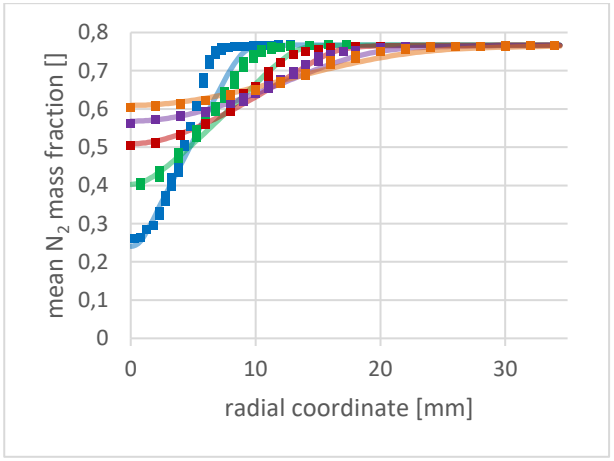

Figure 10. Mean N_2 mass fraction profiles at different heights above the burner.

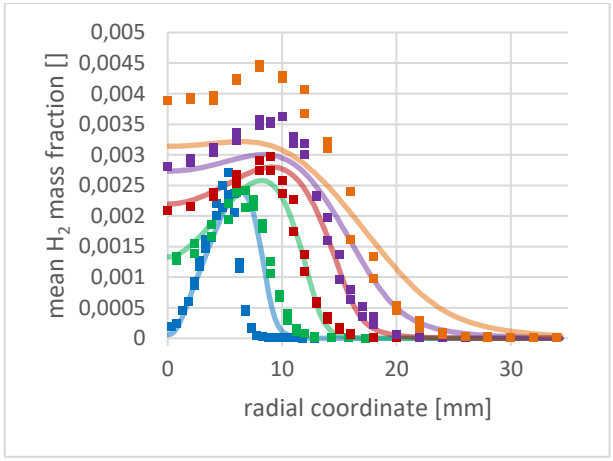

Figure 11. Mean H_2 mass fraction profiles at different heights above the burner.

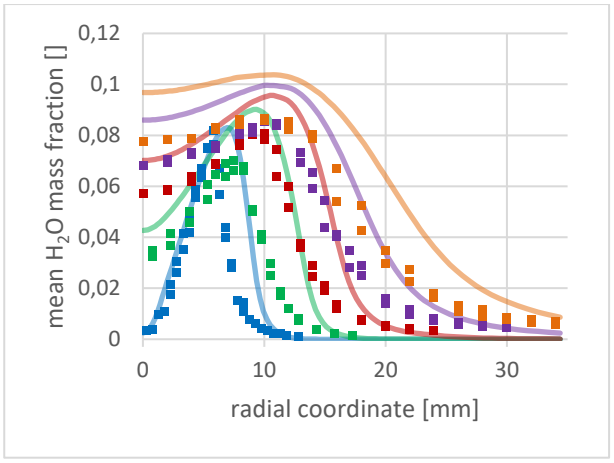

Figure 12. Mean H_2O mass fraction profiles at different heights above the burner.

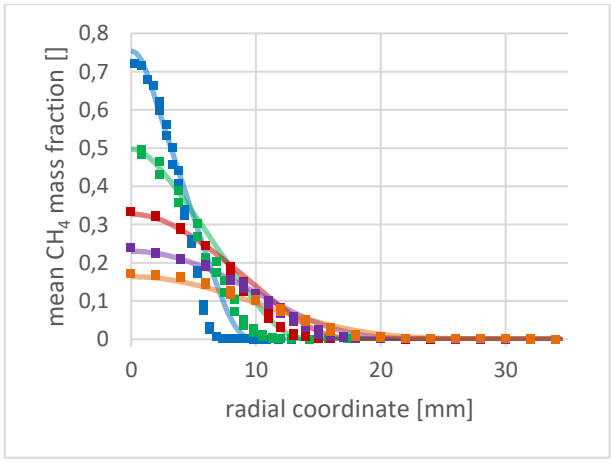

Figure 13. Mean CH_4 mass fraction profiles at different heights above the burner.

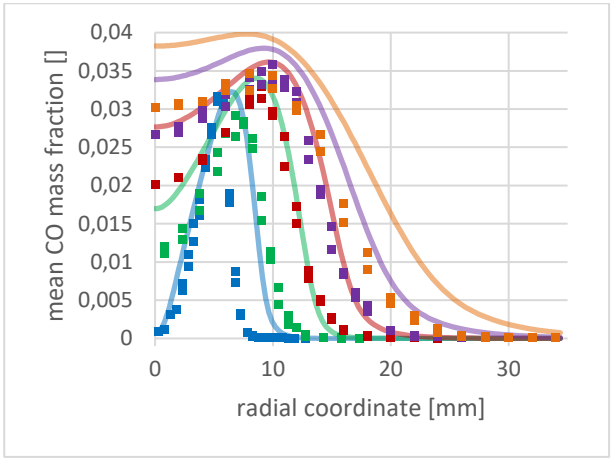

Figure 14. Mean CO mass fraction profiles at different heights above the burner.

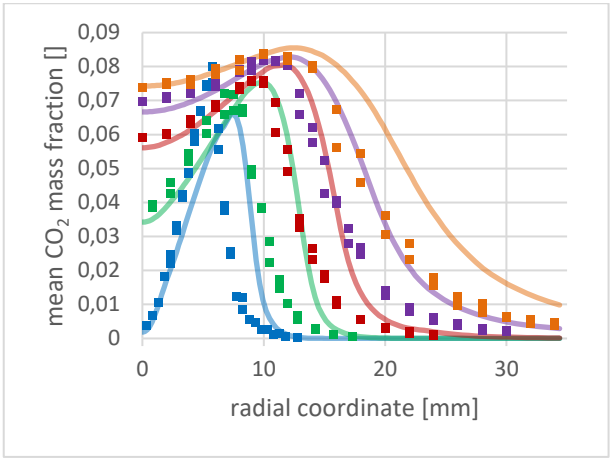

Figure 15. Mean CO_2 mass fraction profiles at different heights above the burner.

The same comments made above for O_2 are pertinent to CO_2.

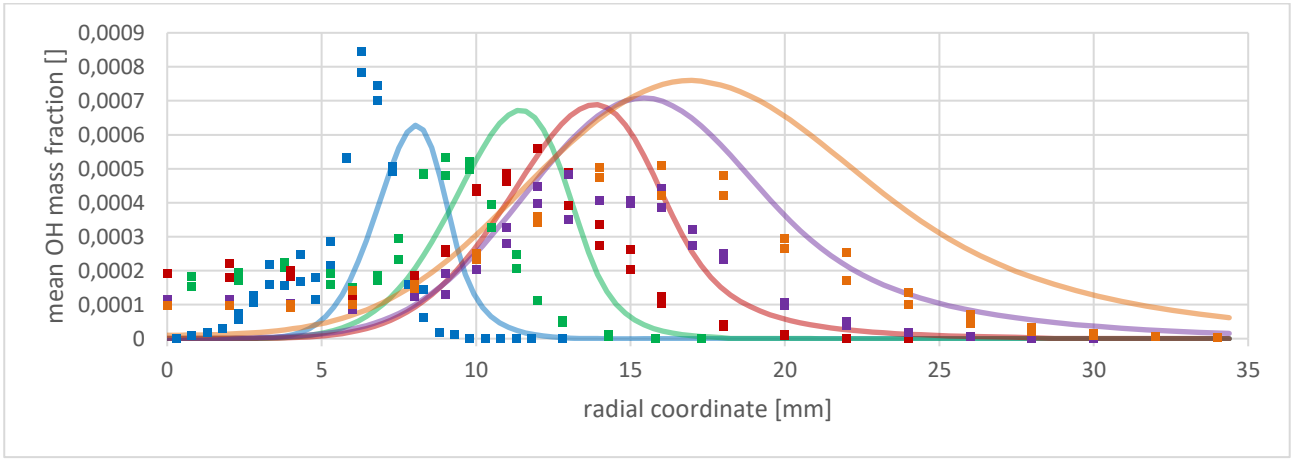

Figure 16. Mean OH mass fraction profiles at different heights above the burner.

From this point onwards, results strongly differed based on which chemical mechanism had been used. For NO, Narayanaswamy, *et al.* (2014) was the one who got closest to the experimental measurements:

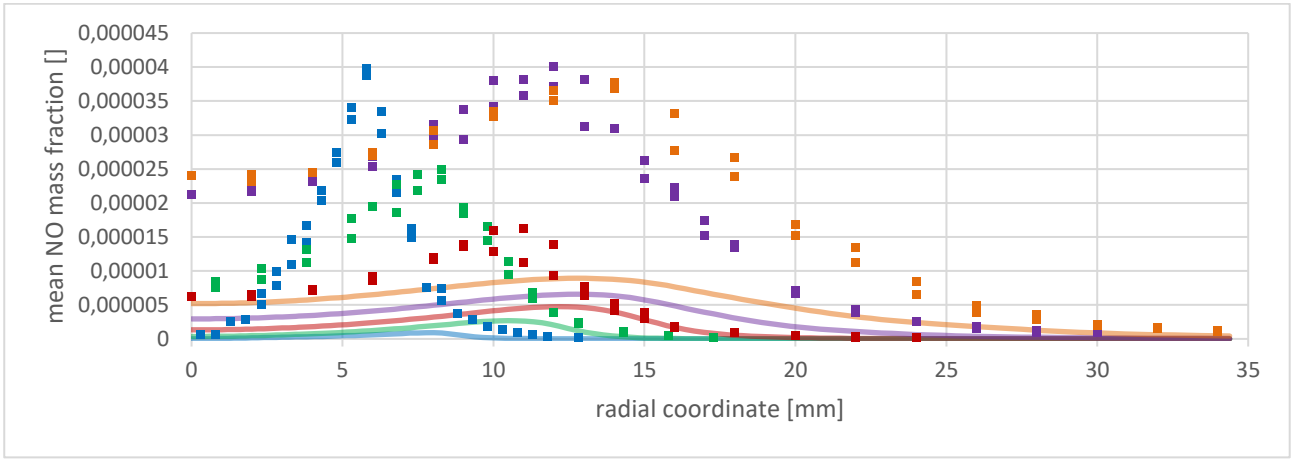

Figure 17. Mean NO mass fraction profiles at different heights above the burner.

But is still inaccurate due to Fluent's missing full TRI. The other mechanisms underpredicted even more the NO concentrations.

Finally, UCSD and Nara's predictions can be considered to have been of similar accuracy for soot, whose experimental measurements were done via Planar *Laser-Induced Incandescence* (LII) (Qamar, *et al.*, 2009):

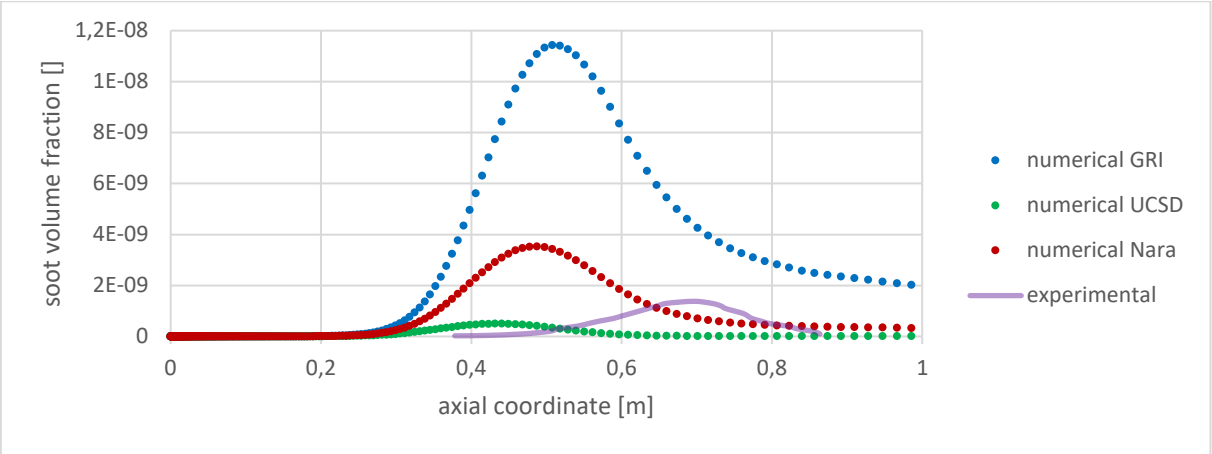

Figure 18. Mean soot volume fraction profiles across the burner's axial distance.

In order to generate the experimental plot in the above graph, it was necessary to visually interpolate from the dashed curve at figure 15 of Qamar, *et al.* (2009) (as their authors did not provide the original measurements in data format).

An independent simulation was carried in a finer mesh (with double the number of cells in the axial direction) and all above results were reproduced, confirming then their grid-converged status. Finally, convergence was also checked against DOM's solid angle discretization (both the number of angles and pixels): results remained unchanged when increasing any of them.

Flame Under Acoustic Forcing

Here lies the greatest frustration of this work: Fluent turned out to be incapable of running *any* transient analysis – i.e. no mention to oscillating boundary conditions yet – from the steady-state, converged SLFM solution… The smaller the time step and more refined the mesh, the quicker the simulation diverged (surprisingly). Switching to a Composition PDF Transport – instead of SLFM – simulation did not help either. Articles about acoustically forced numerical flames have indeed been done so far with in-house CFD codes (e.g. Jocher, *et al.*, 2017) and the authors of the present paper were unable to make Fluent work with that regard.

4. CONCLUSIONS

The present work has attempted to numerically simulate the performance of Delft III Flame under acoustic excitation. Its conclusions can be summarized below:

a) the three mechanisms returned similar results, except for NO mass fraction (where Narayanaswamy, *et al.* was the one who got closest to the experimental measurements, but is still inaccurate due to Fluent's missing full TRI) and for the soot volume fraction (where GRI was the least accurate one);
b) SLFM was sufficient to reach considerably converged results for all variables involved, apart from H_2 and CO mass fractions, which required the additional uSLFM calculation;
c) uSLFM decreased the accuracy of the NO and soot results, pushing them further below from the experimental measurements;
d) increasing the number of moments in MOM did not improve the results;
e) Moss-Brokes returned more accurate results than MOM (due to Fluent's currently lagging implementation of the latter);
f) Fluent was uncappable of successfully running a transient SLFM analysis from a steady-state, converged SLFM solution;
g) Fluent was uncappable of running either a steady-state or a transient Composition PDF Transport analysis from a steady-state, converged SLFM solution.

Further Studies

Further studies on the subject might include:

a) the usage of more precise chemical mechanisms, like Polytechnic University of Milan (Ranzi, *et al.*, 2014) or Narayanaswamy, *et al.*, 2015's complete ones;
b) implementing the full TRI, as described by Habibi, *et al.* (2007);
c) using MOM for the soot calculations, as in Mueller and Pitsch (2012);
d) running a transient SLFM analysis after the steady-state, converged SLFM solution;

e) running both a steady-state and a transient Composition PDF Transport analysis after the steady-state, converged SLFM solution.

5. ACKNOWLEDGMENTS

The support received from Prof. Alex Álisson Bandeira Santos and from the Energy Laboratory's staff at Senai Cimatec is greatly appreciated.

6. REFERENCES

Geuzaine, C., Remacle, J.-F., 2009. "Gmsh: a three-dimensional finite element mesh generator with built-in pre- and post-processing facilities". *International Journal for Numerical Methods in Engineering*, Vol. 79, p. 1309–1331.

Habibi, A., Merci, B., Roekaerts, D., 2007. "Turbulence radiation interaction in Reynolds-averaged Navier–Stokes simulations of nonpremixed piloted turbulent laboratory-scale flames". *Combustion and Flame*, Vol. 151, p. 303–320.

Jocher, A., Foo, K.K., Sun, Z., Dally, B., Pitsch, H., Alwahabi, Z., Nathan, G., 2017. "Impact of acoustic forcing on soot evolution and temperature in ethylene-air flames". *Proceedings of the Combustion Institute*, Vol. 36, p. 781–788.

Kim, I.S., 2004. *Conditional Moment Closure for Non-Premixed Turbulent Combustion*. Ph.D. thesis, University of Cambridge.

Merci, B., Naud, B., Roekaerts, D., 2005. "Flow and Mixing Fields for Transported Scalar PDF Simulations of a Piloted Jet Diffusion Flame ('Delft Flame III')". *Flow Turbulence and Combustion*, Vol. 74, p. 239–272.

Merci, B., Roekaerts, D., Naud, B., 2006. "Study of the performance of three micromixing models in transported scalar PDF simulations of a piloted jet diffusion flame ("Delft Flame III")". *Combustion and Flame*, Vol. 144, p. 476–493.

Mueller, M.E., Pitsch, H., 2012. "LES model for sooting turbulent nonpremixed flames". *Combustion and Flame*, Vol. 159, p. 2166–2180.

Narayanaswamy, K., Pepiot, P., Pitsch, H., 2014. "A chemical mechanism for low to high temperature oxidation of n-dodecane as a component of transportation fuel surrogates". *Combustion and Flame*, Vol. 161, p. 866–884.

Narayanaswamy, K., Pitsch, H., Pepiot, P., 2015. "A chemical mechanism for low to high temperature oxidation of methylcyclohexane as a component of transportation fuel surrogates". *Combustion and Flame*, Vol. 162, p. 1193–1213.

Naud, B., Jiménez, C., Merci, B., Roekaerts, D.J.E.M., 2007. "Transported PDF calculations of the piloted jet diffusion flame 'Delft flame III' with complex chemistry: study of the pilot flame model". In *ECCOMAS Thematic Conference on Computational Combustion 2*. Delft, Netherlands.

Peeters, T.W.J., Stroomer, P.P.J., de Vries, J.E., Roekaerts, D.J.E.M., Hoogendoorn, C.J., 1994. "Comparative experimental and numerical investigation of a piloted turbulent natural-gas diffusion flame". *Symposium (International) on Combustion*, Vol. 25, p. 1241–1248.

Qamar, N.H., Alwahabi, Z.T., Chan, Q.N., Nathan, G.J., Roekaerts, D., King, K.D., 2009. "Soot volume fraction in a piloted turbulent jet non-premixed flame of natural gas". *Combustion and Flame*, Vol. 156, p. 1339–1347.

Ranzi, E., Frassoldati, A., Grana, R., Cuoci, A., Faravelli, T., Kelley, A.P., Law, C.K., 2014. "The CRECK Modeling Group: Complete mechanism". Polytechnic University of Milan.

Reddy, M., De, A., Yadav, R., 2015. "Effect of precursors and radiation on soot formation in turbulent diffusion flame". *Fuel*, Vol. 148, p. 58–72.

Rocha, A.M.A, 2007. *Estudo experimental de chamas difusivas livres turbulentas de gás natural submetidas a oscilações acústicas*. Ph.D. thesis, Universidade Estadual de São Paulo.

Roekaerts, D., Merci, B., Naud, B., 2006. "Comparison of transported scalar PDF and velocity-scalar PDF approaches to 'Delft flame III'". *Comptes Rendus Mécanique*, Vol. 334, p. 507–516.

Santos, A.A.B., Torres, E.A., Pereira, P.A.P., 2011. "Experimental investigation of the natural gas confined flames using the OEC". *Energy*, Vol. 36, p. 1527–1534.

Smith, G.P., Golden, D.M., Frenklach, M., Moriarty, N.W., Eiteneer, B., Goldenberg, M., Bowman, C.T., Hanson, R.K., Song, S., Gardiner Jr., W.C., Lissianski, V.V., Qin, Z. "An optimized mechanism designed to model natural gas combustion".

SNL – Sandia National Laboratories, 2003. Delft III Piloted Natural Gas Flame, International Workshop on Measurements and Computations of Turbulent Non-Premixed Flames.

UCSD – University of California at San Diego, 2016. "Chemical-Kinetic Mechanisms for Combustion Applications".

Yadav, R., Kushari, A., Eswaran, V., Verma, A.K., 2013. "A numerical investigation of the Eulerian PDF transport approach for modeling of turbulent non-premixed pilot stabilized flames". *Combustion and Flame*, Vol. 160, p. 618–634.

7. RESPONSIBILITY NOTICE

The authors are the only responsible for the printed material included in this paper.